Computational Study of Some Hydrogen Bonded Complexes of Water

Teemu Salmi

University of Helsinki
Faculty of Science
Department of Chemistry
Laboratory of Physical Chemistry
A.I. Virtasen aukio 1 (P.O. BOX 55)
FI-00014 University of Helsinki, Finland

Academic Dissertation

To be presented, with the permission of the Faculty of Science of the University of Helsinki, for public discussion in Auditorium A129, Department of Chemistry (A.I. Virtasen aukio 1, Helsinki), on November 16th 2012 at 12 o'clock.

Helsinki 2012

Supervised by:
Prof. Lauri Halonen
Department of Chemistry
University of Helsinki
Helsinki, Finland

Reviewed by:
Prof. Matti Hotokka
Department of Physical Chemistry
Åbo Academi University
Turku, Finland

Prof. Juha Vaara
Department of Physics
University of Oulu
Oulu, Finland

Opponent:
Prof. Marius Lewerenz
Laboratoire Modélisation et
Simulation Multi Echelle
Université Paris-Est
Paris, France

Custos:
Prof. Lauri Halonen
Department of Chemistry

University of Helsinki
Helsinki, Finland

ISBN 978-952-10-8366-2 (paperback)
ISBN 978-952-10-8367-9 (pdf)
http://ethesis.helsinki.fi/
Unigrafia
Helsinki 2012

Abstract

In this thesis, I present calculations of intramolecular vibrational spectra of some hydrogen bonded complexes of water. These include both the water dimer and trimer as well as the water nitric oxide complex. This thesis consists of five research articles. The high-frequency spectrum of the water dimer is studied using an adiabatic model, where the monomer units in the hydrogen bonded complex are treated as individually vibrating molecules. The vibrational eigenvalues are calculated with the variational method. The variationally calculated wave functions are used to obtain the infrared absorption transition intensities. The effect of various corrections, such as the complete basis set expansion, and the counterpoise, core-valence, and the relativistic correction were evaluated in the potential energy surface calculation of the water dimer. A similar vibrational model is used for other complexes. The acceptor tunneling motion, which is a large amplitude mode of the water dimer, was also studied. Finally, the water trimer study is expanded by including the intermolecular potential energy coupling between the monomer units.

Acknowledgements

I thank my supervisor, Professor Lauri Halonen, for giving me an opportunity to work in his research group. I am grateful for you for sharing your knowledge of computational chemistry with me and giving me interesting research projects to work with.

I thank all the the people I have worked with, especially Professor Henrik Kjaergaard, Dr. Vesa Hänninen, and Dr. Nino Runeberg for sharing your expertise with me. I am grateful to my long time officemate Elina Sälli. Our discussions and your advice were really important to my work. I thank Richard Hatz for checking my calculations. I also thank the reviewers, Professor Juha Vaara and Professor Matti Hotokka, for helpful comments regarding my thesis.

I thank the University of Helsinki for the financial support and CSC for providing the computational resources.

I am thankful for all the people, present and former, working in the Laboratory of Physical Chemistry, especially Professor Markku Räsänen, for a nice working environment. I thank everybody who has participated our Friday sähly games and other off work activities. During the years I have had many wonderful officemates. I am grateful to you all for keeping the spirits up during the workdays. All in all, I need to say that the people have made our laboratory a pleasant place to work.

I also thank my non-scientist friends for doing non-scientist things with me. I am also grateful for all of you, especially you Jake, for showing a vast amount of interest towards my work. Anna, thank you for believing in me and supporting me during this process. Finally I thank my parents, Tarja and Simo. Thank you for encouraging me to keep studying.

Teemu Salmi
Helsinki, October 2012

List of Publications

List of Publications Included in the Thesis and the Author's Contributions

This thesis contains the following publications, which are referred to by the Roman numerals I-V:

I. T. Salmi, V. Hänninen, A. L. Garden, H. G. Kjaergaard, J. Tennyson, and L. Halonen. Calculation of the O–H stretching vibrational overtone spectrum of the water dimer, *J. Phys. Chem. A*, 112:6305-6312, 2008. Correction to "Calculation of the O–H stretching vibrational overtone spectrum of the water dimer", *J. Phys. Chem. A*, 116:796-797, 2012.

II. V. Hänninen, T. Salmi, and L. Halonen. Acceptor tunneling motion and O–H stretching vibration overtones of the water dimer, *J. Phys. Chem. A*, 113:7133-7137, 2009.

III. T. Salmi, H. G. Kjaergaard, and L. Halonen. Calculation of overtone O–H stretching bands and intensities of the water trimer, *J. Phys. Chem. A*, 113:9124-9132, 2009.

IV. T. Salmi, N. Runeberg, L. Halonen, J. R. Lane, and H. G. Kjaergaard. Computational Vibrational and Electronic Spectroscopy of the Water Nitric Oxide Complex, *J. Phys. Chem. A*, 114:4835-4842, 2010.

V. T. Salmi, E. Sälli, and L. Halonen. A Nine-dimensional Calculation of the Vibrational OH Stretching and HOH Bending Spectrum of the Water Trimer, *J. Phys. Chem. A*, 116:5368-5374, 2012.

T.S. wrote parts a Fortran program that was used in the variational calculations of the water units in Papers I, III, and IV and the whole program for Paper V. All ab initio calculations in Papers III and V, and most in Paper I were done by T.S. He also wrote the main portion of the manuscripts of Papers III and V and a large part of Paper I. In Paper IV, T.S. performed most the calculations as well as wrote the part of the manuscript that is related to the vibrational problem. In Paper II, the author wrote parts of the manuscript and performed some of the ab initio calculations.

List of Other Publications

1. E. Sälli, T. Salmi, and L. Halonen. Computational high-frequency overtone spectra of the water ammonia complex, *J. Phys. Chem. A*, 115:11594-11605, 2011.

Contents

Chapter 1

Introduction

Water is the single most important molecule for life on the Earth. The oceans cover about 70% of the Earth's surface. Water evaporates from seas and lakes and rains back down in an ongoing process [1]. In the atmosphere, the abundance of water varies between 1 and 2%. More than 99% of the atmosphere, excluding the water vapor, consist of non-polar molecules, namely nitrogen and oxygen. Hence, water is the most common polar molecule in the Earth's atmosphere. This is important because the diatomic non-polar molecules such as N_2 and O_2 do not absorb infrared (IR) radiation. Water molecule is an important IR absorber and crucial to the green house effect. It is also proposed that hydrogen-bonded complexes of water would have a significant effect of the water vapor absorption [2].

Water has many unique properties when compared with similar molecules. For instance, the melting and boiling points are unexpectedly high. For water, these phase transitions appear at higher temperatures than some heavier molecules with similar functional OH group, such as methanol and ethanol. Solid water can possess at least 13 different lattice structures, depending on the temperature and pressure [1]. This is due to the hydrogen bonding between the water molecules. Water is a bent triatomic molecule. The HOH angle is 104.5°. Therefore, it is a dipole. In the solid phase, a single water molecule forms a hydrogen bond with four other water molecules. In liquid water, the average number of the number of hydrogen bonds per molecule is slightly less than four [3]. Most liquid water molecules are arragned in

the tetrahedral formation (four hydrogen bonds) but also other coordination numbers appear [4]. In the gas phase, water molecules can form hydrogen-bonded complexes, such as dimers, trimers, tetramers, etc.

Observing weakly bound complexes is difficult. In the room temperature, the molecules have enough energy to break the hydrogen bonds. Therefore, the experiments are often done at low temperatures. Most of the experimental data are collected using the matrix isolation technique, where the molecules (or complexes) are contained inside a solid matrix. Noble gases are usually used as the matrix substance. The benefit of the matrix isolation method is that the studied complex is not allowed to dissociate. Therefore, it makes a useful method when investigating the hydrogen-bonded complexes water [5–21]. He-droplet experiments are closely related to the matrix isolation ones. The studied molecules are contained inside a cold He-droplet which contains about a few thousands of He atoms. The temperature in the experiments is low enough to make helium liquid [22–24]. Various gas-phase methods have also been used to study these complexes [25–34]. Most of the experimental studies have concentrated on the low-frequency modes, but there are also many high-frequency observations.

The water dimer and trimer have also been studied computationally. Many studies have concentrated on calculating the potential energy surfaces or finding the minimum energy structures [35–42]. As the full variational treatment, which would lead to converged energies for the high-frequency transition overtones, is unfeasible with the current available computational resources, simpler models are developed to obtain both the low- and high-frequency fundamentals [43–45]. The models, where the monomer units are treated as isolated molecules, allow the calculation of both the OH stretching fundamentals and overtones [46–49]. A similar model has been used in this thesis to calculate these transitions. A full variational calculation with an exact kinetic energy operator has been carried out for the monomer units. This thesis consists of five research articles.

In PAPER I, the high-frequency spectrum of the water dimer was calculated. The water dimer was treated as two individually vibrating monomer units. The exact kinetic energy operator was used in the monomer calculations. The coupled cluster method was used to generate the vibrational

potential energy function. The effect of various potential energy surface corrections was studied. The variationally calculated vibrational eigenfunctions were used to compute the transition intensities. Finally some experimental data were used to optimize the potential energy parameters to improve the variational calculation.

The aim of PAPER II was to study the effect the acceptor tunneling motion has on the high-frequency modes. The acceptor tunneling mode is a two-fold motion. It includes the torsional motion and the acceptor wag. An adiabatic model, where the OH stretching Schrödinger equation was solved at different values of the acceptor tunneling coordinates, was used.

The OH stretching and the HOH bending spectrum of the water trimer were calculated in PAPER III. A vibrational model which is similar to the one used in PAPER I was employed. The OH(D) stretching fundamentals as well as the overtones were also calculated up to the third overtone region for all possible fully or partially deuterated isotopologues. The description of the potential energy surface was improved by the least-squares fit to the experimental data.

The high-frequency vibrations of the water nitric oxide complex were calculated up to the second OH and third NO stretching overtone region in PAPER IV using the model from PAPER I. Three conformers had been observed in a matrix isolation study [19]. NO has an unpaired electron, and therefore, it is a radical. The two lowest energy conformers of both possible symmetries of the electronic wave function were studied. The vibrational transition energies and intensities were calculated for H_2O–NO, HDO–NO, and D_2O–NO. The electronic transitions of the water nitric oxide complex were also studied in PAPER IV, but the author was not involved in this part and hence, these are not discussed in this thesis.

PAPER V concentrated on the water trimer. The model that was used in PAPER III was expanded to include some potential energy coupling terms between the monomer units. This, in total nine-dimensional, variational calculation solved a problem related to the hydrogen-bonded OH stretching band shape in PAPER III. The high-frequency spectra up to the OH(D) stretching overtone region of $(H_2O)_3$ as well as the 63 other fully and partially deuterated isotopologues were calculated. The variational calculations were

also performed for another isotopologue of the water trimer, $(H_2^{18}O)_3$.

Chapter 2

Vibrational Calculation

2.1 The Molecular Schrödinger equation

The time-independent non-relativistic Schrödinger equation is formally written as

$$\left(\hat{T} + \hat{V}\right) \Psi = E\Psi, \tag{2.1}$$

where Ψ is the wave function, E is the energy, $\hat{T}$ is the kinetic and $\hat{V}$ is the potential energy operator. Equation 2.1 can also be written as

$$\left(\hat{T}_{\mathrm{N}} + \hat{T}_{\mathrm{e}} + \hat{V}_{\mathrm{N,N}} + \hat{V}_{\mathrm{N,e}} + \hat{V}_{\mathrm{e,e}}\right) \Psi = E\Psi, \tag{2.2}$$

where subindices N and e refer to nuclei and electrons, respectively. The mass of an electron is 9.109×10^{-31} kg, whereas the mass of the lightest nucleus, the proton, is 1.673×10^{-27} kg. Hence, the nuclei are more than 1000 times heavier than the electrons. Therefore, it is a good approximation to assume that the electrons adjust themselves to the nuclear motion, i.e., the electronic part of the wave function has only a parametric dependence on the nuclear configuration. Let us also assume that the wave function can be separated into nuclear (ψ_{N}) and electronic (ϕ_{e}) parts,

$$\Psi = \psi_{\mathrm{N}} \phi_{\mathrm{e}}. \tag{2.3}$$

Using this assumption, the Born-Oppenheimer approximation, we obtain a Schrödinger equation which can be rearranged to

$$\left(\hat{T}_{\mathrm{e}} + \hat{V}_{\mathrm{N,e}} + \hat{V}_{\mathrm{e,e}}\right)\phi_{\mathrm{e}} = \underbrace{\left(E - \frac{\hat{T}_{\mathrm{N}}\psi_{\mathrm{N}}}{\psi_{\mathrm{N}}} - \hat{V}_{\mathrm{N,N}}\right)}_{\approx\text{constant}}\phi_{\mathrm{e}} = E_{\mathrm{e}}\phi_{\mathrm{e}}, \tag{2.4}$$

where E_{e} is the electronic energy. Because, the nuclei are assumed to be stationary, the kinetic energy operator of the nuclei, $\hat{T}_{\mathrm{N}}$, is equal to zero. Several computational methods have been developed to calculate the expectation value for the electronic energy

$$\langle E_{\mathrm{e}}\rangle = \int \mathrm{d}\tau_{\mathrm{e}}\phi_{\mathrm{e}}^{*}\left(\hat{T}_{\mathrm{e}} + \hat{V}_{\mathrm{N,e}} + \hat{V}_{\mathrm{e,e}}\right)\phi_{\mathrm{e}}. \tag{2.5}$$

The nuclear repulsion term, $\hat{V}_{\mathrm{N,N}}$, is usually included in the calculation of the electronic energy.

2.2 The Electronic Energy

Electrons are fermions. Therefore, the electronic wave function is antisymmetric with respect to the permutation of two electrons

$$\phi_{\mathrm{e}}(\ldots \mathrm{e}_i \ldots \mathrm{e}_j \ldots) = -\phi_{\mathrm{e}}(\ldots \mathrm{e}_j \ldots \mathrm{e}_i \ldots). \tag{2.6}$$

In an n-electron system, this condition is met using the Slater determinant as the trial function

$$\phi_{\mathrm{e}}(\mathrm{e}_1, \mathrm{e}_2 \ldots \mathrm{e}_n) = \frac{1}{\sqrt{n!}}\begin{vmatrix} \chi_1(\mathrm{e}_1) & \chi_2(\mathrm{e}_1) & \cdots & \chi_n(\mathrm{e}_1) \\ \chi_1(\mathrm{e}_2) & \chi_2(\mathrm{e}_2) & \cdots & \chi_n(\mathrm{e}_2) \\ \vdots & \vdots & \ddots & \vdots \\ \chi_1(\mathrm{e}_n) & \chi_2(\mathrm{e}_n) & \cdots & \chi_n(\mathrm{e}_n) \end{vmatrix}, \tag{2.7}$$

where χ_i are atomic spin-orbitals [50].

The basis of the electronic structure calculations is the Hartree-Fock method, where an n-electron problem is separated into n one electron problems. The electronic wave function is represented by a single Slater determinant. The problem can be reduced into a set of one-electron eigenvalue equations [51]

$$\left(\hat{T}_{\mathrm{e}_i} + \sum_{\alpha=1}^{N}\hat{V}_{\mathrm{N,e}_i} + v_{\mathrm{HF}}(i)\right)\chi_i = \epsilon_i\chi_i. \tag{2.8}$$

An electron interacts with the other ones only via the average field caused by the other electrons, $v_{\mathrm{HF}}(i)$. First, an initial guess for the spin orbitals is made. It is used to calculate $v_{\mathrm{HF}}(i)$. A better estimate for the spin orbitals is obtained when the eigenvalue equations are solved. $v_{\mathrm{HF}}(i)$ is recalculated using the new spin orbitals. This process is repeated, until the calculation has converged [51]. These spin orbitals are used to construct the Slater determinant, which is the Hartree-Fock ground state wave function. Let us mark the solution with $|\mathrm{HF}\rangle$. The error in the energy expectation value that is calculated using the Hartree-Fock method (E_{HF}) is usually less than 1% [50].

The correlation energy, E_{corr}, is defined as

$$E_{\mathrm{corr}} = E_{\mathrm{exact}} - E_{\mathrm{HF}} \tag{2.9}$$

where E_{exact} is the exact energy of the system. The correlation energy needs to be included in the calculations when accurate energies are needed. A better value for the electronic energy is obtained by including more Slater determinants to the model. In these added determinants, one or more electrons are excited to virtual orbitals. The best possible solution would be obtained if all the possible excitations were included in the model. However, this procedure would lead, in most cases to unnecessarily long and computationally demanding calculations. The series needs to be truncated. The choice of the truncation method is not necessarily unambiguous. Different approaches to the problem have been made. These include, for instance: the Møller-Plesset perturbation theory (MP), the configuration interaction (CI), and the coupled cluster (CC) method [50].

In the case of small molecules with less than ten atoms, the coupled cluster approach has proven to be the most efficient method to study the electronic energy. The coupled cluster wave function is obtained from the Hartree-Fock wave function by using the cluster operator [50]

$$|\mathrm{CC}\rangle = e^{\hat{T}}|\mathrm{HF}\rangle, \tag{2.10}$$

where the cluster operator is a sum of the excitations

$$\hat{T} = \hat{T}_1 + \hat{T}_2 + \ldots \hat{T}_n, \tag{2.11}$$

where $\hat{T}_i$ contains all terms where i electrons are excited. The coupled cluster method with single, double, and perturbative triple excitations, CCSD(T), is capable of producing the electronic energies, which are accurate enough for the purpose of this work. It is used to obtain all the potential energy and dipole moment surfaces in this work.

Another feature, besides the computational method that affects the quality of the electronic structure calculations is the basis set. The form of the actual wave function is unknown. A usual way to overcome this problem is expressing the wave function as a sum of simpler functions: the basis functions. In principle, any set of orthonormal functions would suit. A smart choice of the basis set can decrease the computational cost of the electronic structure calculations. The aim is to mimic the true wave function of a molecule as closely as possible. Unfortunately, the only system that can be solved analytically without the Born-Oppenheimer approximation contains one electron and one nucleus. The radial part of the solution has the form [52]

$$f(\rho)e^{-\zeta\rho}, \tag{2.12}$$

where ρ is the distance from the nucleus to the electron, $f(\rho)$ is a polynomial of ρ, and ζ is a parameter. However, a function of this form is inconvenient due to the high computational cost of the integrals. It is computationally more suitable to use Gaussian functions

$$g(\rho)e^{-\beta\rho^2}, \tag{2.13}$$

as the radial part. The hydrogenic functions (Equation 2.12) can be expressed as linear combinations of Gaussian functions. The angular part consists of the spherical harmonics.

In quantum chemistry, the aim is to calculate the properties of molecules. The atomic basis functions cannot necessarily describe the bonding properly. Therefore, some additional functions are included into the basis sets. Polarization functions are Gaussians with a higher angular momentum than the occupied atomic orbitals. These make the basis set more versatile in describing the bonding. Another group of functions that is often included into the basis sets is the diffuse functions. These are functions of a small value of β (Equation 2.13). Therefore, these functions decay slowly and therefore have

a long range. The diffuse functions are used to better describe the long range interactions such as the hydrogen bonding [50].

In this work, all ab initio calculations are performed using the *correlation consistent polarized valence X zeta*, cc-pVXZ or aug-cc-pVXZ, basis sets by Dunning [53, 54]. The aug- prefix indicates that the diffuse functions are included into the basis set. The symbol X stands for the number of ζ values, which are described as linear combinations of Gaussian functions that is included in the basis set. These are obtained by minimizing the correlation energy. Therefore, these functions are well suited for high-level, such as coupled cluster, calculations.

In the electronic structure calculations, it is often customary not to correlate the core electrons. In the case of the water molecule, this concerns the two 1s-electrons of the oxygen atom. When the effect of the core electron correlation is calculated, a different basis set needs to be used. Therefore, the aug-cc-pCVXZ basis sets [55] have been developed.

2.3 The Nuclear Schrödinger equation

The potential energy surface (PES) for the nuclear motion is calculated using Equation 2.5 with different nuclear geometries. Finally, the vibration-rotation Schrödinger equation is

$$\left(\hat{T}_{\mathrm{N}} + \langle E_{\mathrm{e}} \rangle + \hat{V}_{\mathrm{N,N}}\right) \psi_{\mathrm{N}} = \left(\hat{T}_{\mathrm{N}} + \hat{V}_{\mathrm{N}}\right) \psi_{\mathrm{N}} = E \psi_{\mathrm{N}}. \tag{2.14}$$

There are $3N$ degrees of freedom in a molecule containing N atoms. In the absence of an external potential, the molecule can move freely. Hence, the three translational degrees of freedom are separated from the other motions. The rotational and vibrational motions are coupled with each others. The vibrational contribution determines the center of the transition band and the rotational part gives the band its fine structure. In this work, the main interest is in locating the band center of the transition, and only transitions without the rotational contribution are included. Now we are left with

$$3N - 3 \times \text{translation} - 3 \times \text{rotation} = 3N - 6 \tag{2.15}$$

internal vibrational coordinates.[1] A natural choice for the coordinates are the bond lengths, bond angles and dihedral angles. Sometimes, depending on the system, symmetry coordinates can be used to obtain a faster convergence in the vibrational calculation. That is, for instance, in the case of ammonia [56].

2.3.1 The Vibrational Kinetic Energy Operator

The vibrational kinetic energy operator is a purely quantum mechanical entity. It can be derived completely and exactly in any coordinate system using a pen and paper [57]. The only parameters needed are the Planck constant divided by 2π, $\hbar = \frac{h}{2\pi}$, and the masses of the nuclei.

In a general case, the kinetic energy operator is expressed in Cartesian coordinates

$$\hat{T}_{\mathrm{N}} = -\frac{\hbar^2}{2} \sum_{\alpha=1}^{N} \frac{\nabla_\alpha^2}{m_\alpha}, \tag{2.16}$$

where α refers to the nuclei, N is the number of nuclei, m_α is the mass of the atom α, and the Laplacian is $\nabla_\alpha^2 = \frac{\partial^2}{\partial x_\alpha^2} + \frac{\partial^2}{\partial y_\alpha^2} + \frac{\partial^2}{\partial z_\alpha^2}$. However, in many cases, the Cartesian coordinates are not a convenient set. Equation 2.16 also includes the translational and rotational motions. We can express the kinetic energy operator in the internal coordinates (q_i), i.e., excluding the translation and rotation, as [58]

$$\hat{T}_{\mathrm{int}} = -\frac{\hbar^2}{2} \sum_{i,j=1}^{3N-6} \left(\frac{\partial}{\partial q_i} + \frac{1}{J} \frac{\partial J}{\partial q_i} \right) g^{(q_i,q_j)} \frac{\partial}{\partial q_j}, \tag{2.17}$$

where J is the Jacobian of the coordinate transformation [57] and the mass weighted reciprocal metric tensor elements are

$$g^{(q_i,q_j)} = \sum_{\alpha=1}^{N} \frac{1}{m_\alpha} \left(\nabla_\alpha q_i\right) \cdot \left(\nabla_\alpha q_j\right). \tag{2.18}$$

The g-tensor values at the potential energy minimum geometry are the Wilson g-matrix elements [59]. The kinetic energy operator can be changed into

[1] In a linear molecule, there are only two rotational degrees of freedom, and therefore, $3N - 5$ vibrational coordinates.

a form which is easier to handle by transforming the wave function

$$\psi = \psi' J^{-\frac{1}{2}}. \tag{2.19}$$

By doing so, the integrals can be calculated as

$$T_{vv'} = \int \mathrm{d}\tau \psi_{v'}^* \hat{T}_{\mathrm{int}} \psi_v = \int J \mathrm{d}q_1 \mathrm{d}q_2 \ldots \mathrm{d}q_{3N-6} \psi_{v'}'^* J^{-\frac{1}{2}} \hat{T}_{\mathrm{int}} \psi_v' J^{-\frac{1}{2}} =$$

$$-\frac{\hbar^2}{2} \int \mathrm{d}q_1 \mathrm{d}q_2 \ldots \mathrm{d}q_{3N-6} \psi_{v'}'^* \sum_{i,j=1}^{3N-6} \left(g^{(q_i,q_j)} \frac{\partial^2}{\partial q_i \partial q_j} + \frac{\partial g^{(q_i,q_j)}}{\partial q_i} \frac{\partial}{\partial q_j} + V'(q_i,q_j) \right) \psi_v', \tag{2.20}$$

where

$$V'(q_i,q_j) = \frac{1}{4} \frac{\partial J}{\partial q_i} \frac{\partial J}{\partial q_j} g^{(q_i,q_j)} J^{-2} - \frac{1}{2} \frac{\partial^2 J}{\partial q_i \partial q_j} g^{(q_i,q_j)} J^{-1} - \frac{1}{2} \frac{\partial g^{(q_i,q_j)}}{\partial q_i} \frac{\partial J}{\partial q_j} J^{-1} \tag{2.21}$$

does not include wave function derivatives. Therefore, V' is called the *pseudopotential* term. At least in the case of the water molecule, this term has little effect on the results and can be neglected [PAPER V]. Hence, the Jacobian needs not to be known.

2.3.2 The Potential Energy Operator

The potential energy operator, $\hat{V}_{\mathrm{N}}$, from Equation 2.14 determines the environment where the particles move. It is a function of the internal coordinates q_i. It is convenient to express such a function as a Taylor series expansion

$$\hat{V}_{\mathrm{N}}(q_1, q_2, \ldots, q_{3N-6}) = \sum_{i_1,i_2,\ldots,i_{3N-6}=0} \left. \frac{\partial^{i_1+i_2+\ldots+i_{3N-6}} V}{\partial q_1^{i_1} \partial q_2^{i_2} \ldots \partial q_{3N-6}^{i_{3N-6}}} \right|_{\Delta q=0} \frac{\Delta q_1^{i_1} \Delta q_2^{i_2} \ldots \Delta q_{3N-6}^{i_{3N-6}}}{i_1!, i_2!, \ldots, i_{3N-6}!}, \tag{2.22}$$

where $\Delta q_i = q_i - q_i^{\mathrm{e}}$ and the superscript e refers to a reference geometry. The potential energy function is a combination of the attractive force caused by the electrons and the repelling of the nuclei. At some nuclear configurations, these forces are in balance, i.e., the first derivatives of the potential energy function with respect to the internal coordinates are all equal to zero. If the second derivatives are positive, this kind of point is a minimum. It is convenient to choose the global minimum energy structure as the reference geometry.

The potential energy function depends on the electronic structure of the molecule. Therefore, the electronic energy of the system needs to be known in order to determine $\hat{V}_{\mathrm{N}}$. An ab initio method is used to calculate it in this work. The energy is calculated at certain nuclear geometries and it is fitted to an analytical function from Equation 2.22. Another option to determine the coefficients in Equation 2.22 is to use experimental data.

2.4 Solving the Vibrational Schrödinger Equation

The simplest vibrational system is a diatomic molecule. Only one vibrational coordinate, the bond length (r), is needed to describe the vibrational problem. The only reciprocal metric tensor element is a constant, $g^{(r,r)} = \frac{1}{\mu}$, where μ is the reduced mass of the molecule. The lowest level approximation is to use only the harmonic potential, which results in the Schrödinger equation

$$\hat{H}\psi' = -\frac{\hbar^2}{2\mu}\frac{\mathrm{d}^2\psi'}{\mathrm{d}r^2} + \frac{1}{2}f_2\left(r - r_{\mathrm{e}}\right)^2\psi' = E\psi', \tag{2.23}$$

where f_2 is the harmonic force constant and r_{e} is the equilibrium bond length. It can be solved analytically with the eigenvalues

$$E_v = \left(v + \frac{1}{2}\right)\hbar\omega, \qquad \text{where } \omega = \sqrt{\frac{f_2}{\mu}} \text{ and } v = 0, 1, 2\ldots \tag{2.24}$$

Using this model, the energy difference between consecutive energy levels is constant. Even though the harmonic approximation produces fundamental transition energies which are in a reasonable agreement with some experimental results, it still misses some key properties of the observed vibrational spectrum:

(1) **Anharmonicity.** The energy difference of two consecutive energy levels $(E_v - E_{v-1})$ decreases as v increases.

(2) **Dissociation.** When a bond stretching mode absorbs enough energy, the bond dissociates.

These features cannot be reproduced computationally unless anharmonicity is included into the potential energy operator. It can be done by including

high order terms in the potential energy function. Another option is to use an anharmonic potential energy function that is not a Taylor series expansion. A popular choice is to use the Morse potential

$$\hat{V}_{\mathrm{N}} = D_e y^2, \qquad \text{where } y = 1 - \exp\left(1 - a\Delta r\right). \tag{2.25}$$

The quantities D_e and a are the Morse parameters [60]. The Morse potential is anharmonic and it has the right kind of asymptotic behavior at large displacements. The eigenvalue solution for the Morse oscillator Schrödinger equation is

$$E_v = \left(v + \frac{1}{2}\right)\hbar\omega - \left(v + \frac{1}{2}\right)^2 \hbar\omega x, \qquad \text{where } \omega = \sqrt{\frac{2a^2 D_e}{\mu}} \text{ and } \omega x = \frac{a^2\hbar}{2\mu}. \tag{2.26}$$

Because ωx is always positive, the anharmonicity pushes the vibrational energies closer to each others when v is increased. Therefore, the energy difference between two consecutive energy levels decreases when anharmonicity is introduced to the system. The flexibility of the potential energy function can be increased by adding higher order terms into the potential energy function. In this work, a series expansion of the Morse variable has been used to improve the least-squares optimization of the potential energy parameters. In general, the second-order term (Equation 2.25) is the most important one and the rest are fine tuning of the fit.

For the water molecule, three vibrational coordinates are needed. In this work, two OH bond lengths and the HOH bending angle are used. The kinetic energy operator from Equation 2.17 is used. The reciprocal metric tensor elements for a bent triatomic molecule are well known in the literature [59]. The potential energy function contains one- and two-dimensional parts. This kind of a problem cannot be solved analytically. The variational method was used in this work to solve the water monomer Schrödinger equation.

2.4.1 The Variational Method

When both the kinetic and the potential energy operators have been obtained, the vibrational Schrödinger equation can be solved. The variational method is a powerful tool in solving vibrational problems. However, the use

of variational method is limited to small molecules because the demand for the computational resources increases rapidly as the number of the vibrational degrees of freedom increases.

The variational method is based on the principle which states that *the energy calculated using any trial function is always greater or equal with the exact ground state energy* [52]. The usual choice for the trial wave function is a linear combination of basis functions, which are products of eigenfunctions of one-dimensional Hermitian operators. Solving the Schrödinger equation can be reduced into an eigenvector problem, where the Hamiltonian matrix, which consists of elements

$$\mathbf{H}_{mn} = \langle m|\hat{H}|n\rangle, \tag{2.27}$$

is diagonalized. Here m and n refer to basis functions, which are products of the one-dimensional functions. The smallest eigenvalue of the Hamiltonian matrix is the energy of the vibrational ground state. The corresponding eigenvector contains the coefficients that determine the ground state wave function. The matrix diagonalization also produces wave functions which are orthogonal with the calculated ground state wave function and obviously each others. Hence, these functions are also eigenfunctions of the Hamiltonian and the corresponding eigenvalues are vibrational energies of the molecule in question.

2.4.2 Adiabatic Approximation

The variational method is a good method in calculating the vibrational term values of small molecules. The most time-consuming part in the variational calculation is the diagonalization of the Hamiltonian matrix. Because the basis set is expressed as a series, the number of basis functions increases rapidly when the molecule gets larger. For a basis set consisting of M functions, an $(M \times M)$ matrix needs to be diagonalized. This sets some serious limits to the size of the studied molecule. Let us consider a system with p vibrational degrees of freedom. If m one-dimensional basis functions, $\psi_{i,j}$, are needed to describe each vibrational mode, the variational calculation contains the

p-dimensional basis functions

$$\begin{aligned}
\Psi_{11\ldots1} &= \psi_{1,1}\psi_{2,1}\ldots\psi_{p,1} \\
\Psi_{21\ldots1} &= \psi_{1,2}\psi_{2,1}\ldots\psi_{p,1} \\
&\vdots \\
\Psi_{mm\ldots m} &= \psi_{1,m}\psi_{2,m}\ldots\psi_{p,m}.
\end{aligned} \tag{2.28}$$

The total number of these basis functions is m^p. The usual matrix diagonalization routines scale as M^3. Therefore, the required CPU time of the variational calculation scales as m^{3p}, i.e., it depends exponentially on the number of vibrational degrees of freedom. Hence, it is important to keep the number of degrees of freedom as low as possible.

The water dimer consists of six atoms. There are eight equivalent minimum energy geometries separated by low barriers in the potential energy surface, which makes the complex floppy. Therefore, a full variational calculation of the water dimer would not be feasible using the current computational resources.

The vibrational modes of the water dimer can be divided into two groups: six low-frequency modes (below 1000 cm^{-1}) involve mostly the intermolecular motions of the monomer units and six high-frequency modes (1500 – 3800 cm^{-1}) are the deformation of the water units. A similar division can be made in the case of all complexes studied in this thesis. Before the complex is formed, only six high-frequency modes (three in both water molecules) exist. When the two water molecules combine and form the water dimer, the number of vibrational modes increases to $3 \times 6 - 6 = 12$. The six additional modes are intramolecular vibrational modes. In these motions, the water monomer units remain almost fixed.

If the energy difference between vibrational modes is large, the motions can be separated in the Schrödinger equation using the adiabatic approximation, which is similar to the Born-Oppenheimer approximation. The low-frequency modes are kept fixed when the high-frequency wavenumbers and wave functions are calculated. In this work, the vibrational coupling between the monomer units in the water dimer, water trimer, and water nitric oxide complex is assumed to be insignificant [PAPERS I, III, and IV]. Hence, the monomer units have been treated as individually vibrating wa-

ter or nitric oxide molecules in an external potential caused by the other monomer units. This treatment is sufficient in obtaining the big picture in the OH stretching domain. However, it lacks the observed fine structure of the hydrogen-bonded OH stretching spectrum of the water trimer. The treatment of the water trimer has been improved by including the intermolecular OH stretching coupling in the model [PAPER V]. Due to the longer distance between the free OH stretching modes, the intermolecular coupling has little effect in the calculated free OH stretching spectrum at 3700 – 3730 cm^{-1}.

Let us consider an A–B complex.[2] The internal coordinates of the monomer unit A are defined using only atoms belonging to the monomer unit A. The same applies for B. All the terms in the internal coordinate kinetic energy operator, given in Equation 2.17, depend on the g-tensor (Equation 2.18). As the monomer units A and B do not share any atoms, all the g-tensor elements that would directly couple the internal coordinates of A and B are equal to zero. Therefore, the kinetic energy operator of the complex ($\hat{T}_{\mathrm{complex}}$) can be divided into three parts

$$\hat{T}_{\mathrm{complex}} = \hat{T}_{\mathrm{A}} + \hat{T}_{\mathrm{B}} + \hat{T}_{\mathrm{inter}}, \tag{2.29}$$

where $\hat{T}_{\mathrm{A}}$ and $\hat{T}_{\mathrm{B}}$ include derivates only with respect to the internal coordinates of the monomer unit A and B, respectively, and $\hat{T}_{\mathrm{inter}}$ includes the intermolecular degrees of freedom and their coupling with the monomer units. In this work, in PAPERS I, III, IV, and V, the intermolecular coordinates are fixed to their minimum energy geometry values. Therefore, all derivatives with respect to them are constrained to zero, and

$$\hat{T}_{\mathrm{inter}} = 0. \tag{2.30}$$

A Taylor series expansion (Equation 2.22) is used as the potential energy operator. All the potential energy surface coefficients that include any of the intermolecular modes are constrained to zero in the adiabatic approximation used in this work. The terms in the potential energy series can be rearranged so that

$$\hat{V}_{\mathrm{complex}} = \hat{V}_{\mathrm{A}} + \hat{V}_{\mathrm{B}} + \hat{V}_{\mathrm{AB}}, \tag{2.31}$$

[2]The equations that are derived here can be expanded to larger complexes, e.g., the water trimer.

where $\hat{V}_{\mathrm{A}}$ and $\hat{V}_{\mathrm{B}}$ include only the internal coordinates of A and B, respectively, and $\hat{V}_{\mathrm{AB}}$ consists of terms that couple A and B. Now the Hamiltonian for the complex can be written as

$$\hat{H}_{\mathrm{AB}} = \left(\hat{T}_{\mathrm{A}} + \hat{V}_{\mathrm{A}}\right) + \left(\hat{T}_{\mathrm{B}} + \hat{V}_{\mathrm{B}}\right) + \hat{V}_{\mathrm{AB}} \tag{2.32}$$

or in the case of a three body complex, A–B–C

$$\hat{H}_{\mathrm{ABC}} = \left(\hat{T}_{\mathrm{A}} + \hat{V}_{\mathrm{A}}\right) + \left(\hat{T}_{\mathrm{B}} + \hat{V}_{\mathrm{B}}\right) + \left(\hat{T}_{\mathrm{C}} + \hat{V}_{\mathrm{C}}\right) + \hat{V}_{\mathrm{ABC}} \tag{2.33}$$

The intermolecular coupling between the monomer units is weak. If it is assumed to be zero, the Hamiltonian in Equation 2.32 can be separated into two parts which depend only on a single monomer unit

$$\begin{aligned} \hat{H}_{\mathrm{A}} &= \hat{T}_{\mathrm{A}} + \hat{V}_{\mathrm{A}} \\ \hat{H}_{\mathrm{B}} &= \hat{T}_{\mathrm{B}} + \hat{V}_{\mathrm{B}}. \end{aligned} \tag{2.34}$$

Whether the intermolecular coupling is significant or not depends on the system and the accuracy that is needed. In the cases of the water dimer and the water nitric oxide complex, it was unnecessary to include it. However, the uncoupled model was unable to reproduce the observed hydrogen-bonded OH stretching band shape of the water trimer in PAPER III. Therefore, the Hamiltonian from Equation 2.33 was used in PAPER V.

The effect that the large amplitude motions have on the high-frequency modes can be evaluated using an adiabatic model. In the case of the water dimer, the OH stretching modes were calculated as a function of the acceptor tunneling motion in PAPER II. The harmonic force constant of the OH stretching mode was calculated at various values of the acceptor tunneling coordinate ξ. A one-dimensional model for the OH stretching modes was used. The Hamiltonian was constructed, and the corresponding Schrödinger equation

$$\hat{H}_{\mathrm{OH}}[\xi]\psi_{\mathrm{OH}} = E[\xi]\psi_{\mathrm{OH}} \tag{2.35}$$

was solved at various different values of the acceptor tunneling coordinate. Here, the notation $[\xi]$ denotes the parametric dependence on ξ.

2.4.3 Calculating the Transition Intensities

In the observed spectrum the peaks, have two features. On one hand, there is the transition energy, and, on the other hand, the transition intensity. The intensity can be described as the transition probability from the ground state to an excited one. A dimensionless oscillator strength ($f_{\mathrm{e}\leftarrow\mathrm{g}}$) can be used as a measure of the transition intensity [61]

$$f_{\mathrm{e}\leftarrow\mathrm{g}} = 4.70 \times 10^{-7} \left[\mathrm{cm\ D}^{-1}\right] \tilde{\nu}_{\mathrm{e}\leftarrow\mathrm{g}} \left|\langle \mathrm{e}|\vec{\mu}|\mathrm{g}\rangle\right|^2 . \tag{2.36}$$

Its magnitude depends on the transition wavenumber, $\tilde{\nu}_{\mathrm{e}\leftarrow\mathrm{g}}$, and the integral $|\langle \mathrm{e}|\vec{\mu}|\mathrm{g}\rangle|^2$ where e and g refer to the excited and ground states, respectively, and $\vec{\mu}$ is the molecular dipole moment vector as a function of the internal coordinates.

All dipole moments in this work have been calculated using the finite field method. In the case of small electric fields, the dipole moment vector can be expressed as [62]

$$\vec{\mu}_i = -\left(\frac{\partial E}{\partial \varepsilon_i}\right)_{\varepsilon_i=0} \hat{\mathbf{e}}_i \approx -\frac{\Delta E}{\Delta \varepsilon_i}\hat{\mathbf{e}}_i, \qquad i = x, y, \text{ or } z \tag{2.37}$$

where E is the energy of the system as a function of the electric field $\vec{\varepsilon}$ and $\hat{\mathbf{e}}_x$, $\hat{\mathbf{e}}_y$, and $\hat{\mathbf{e}}_z$ are the Cartesian unit vectors. Let ϵ be a weak electric field. The energy of the studied molecule is calculated in the presence of electric fields. The dipole moment vector can be expressed in three dimensions as

$$\vec{\mu} = -\frac{E(\epsilon\hat{\mathbf{e}}_x) - E(-\epsilon\hat{\mathbf{e}}_x)}{2\epsilon}\hat{\mathbf{e}}_x - \frac{E(\epsilon\hat{\mathbf{e}}_y) - E(-\epsilon\hat{\mathbf{e}}_y)}{2\epsilon}\hat{\mathbf{e}}_y - \frac{E(\epsilon\hat{\mathbf{e}}_z) - E(-\epsilon\hat{\mathbf{e}}_z)}{2\epsilon}\hat{\mathbf{e}}_z. \tag{2.38}$$

The dipole moment vector is calculated at various geometries. After performing a least squares optimization of the dipole moment parameters, the dipole moment function is obtained as a function of the internal coordinates. A Taylor series expansion is used as the dipole moment function in this work.

In general, the choice of the dipole moment axes is arbitrary. This is true in a full dimensional variational calculation, which also includes the rotational degrees of freedom. An Eckart axis system is developed to minimize the effect of rotation [63]. It is crucial when calculating the transition intensities of some molecules, for instance, ammonia [56]. However, in the case of water the

observed absorption intensities can be reproduced with a reasonable accuracy using fixed dipole moment axes.

In this work, the rotational motion has been ignored. Hence, the intensities that are calculated using Formula 2.36 are sums of the intensities of the vibration-rotation peaks that can be observed experimentally. This means that if the rotational degrees of freedom would be included into the model, the total intensity of a rovibrational band would be approximately equal to the vibrational model.

Chapter 3

The Hydrogen Bonded Complexes

Let us consider a molecular system X–H$\cdots$Y. A hydrogen bond can be formed between a hydrogen atom and an electronegative fragment (Y). Three points are made of such complexes in Reference [64]: (1) the X–H bending wavenumber increases, (2) the X–H stretching wavenumber decreases, and (3) the band width and the intensity of the X–H stretching transition increase. As a hydrogen bond is created, the X–H bond becomes weaker. The unit that donates the hydrogen atom into the hydrogen bond, X–H, is often referred as the "donor" unit whereas the electronegative fragment accepting the hydrogen atom is the "acceptor" unit. Spectroscopically, the donor unit is often more interesting than the acceptor unit because the biggest changes appear in the bonded X–H stretching oscillator. The free and bonded OH stretching potential energy curves of the monomer unit 1 of the water trimer are presented in Figure 3.1. When the free OH (OH_f) stretching coordinate is displaced from the minimum, the potential energy curve increases more steeply than in the corresponding bonded OH (OH_b) stretching surface. This is due to the attraction between the electronegative acceptor unit and the positively charged proton. Therefore, the OH_b bond is longer than the corresponding OH bond in an isolated molecule. The electronegativity difference of the X and Y fragments determines the strength of the hydrogen bond. In one extreme limit, the X and Y fragments are the same. An example of this is the $H_5O_2^+$ molecule where a proton forms a bridge between two water molecules. The two water molecules are located in the symmetrical positions of the complex.

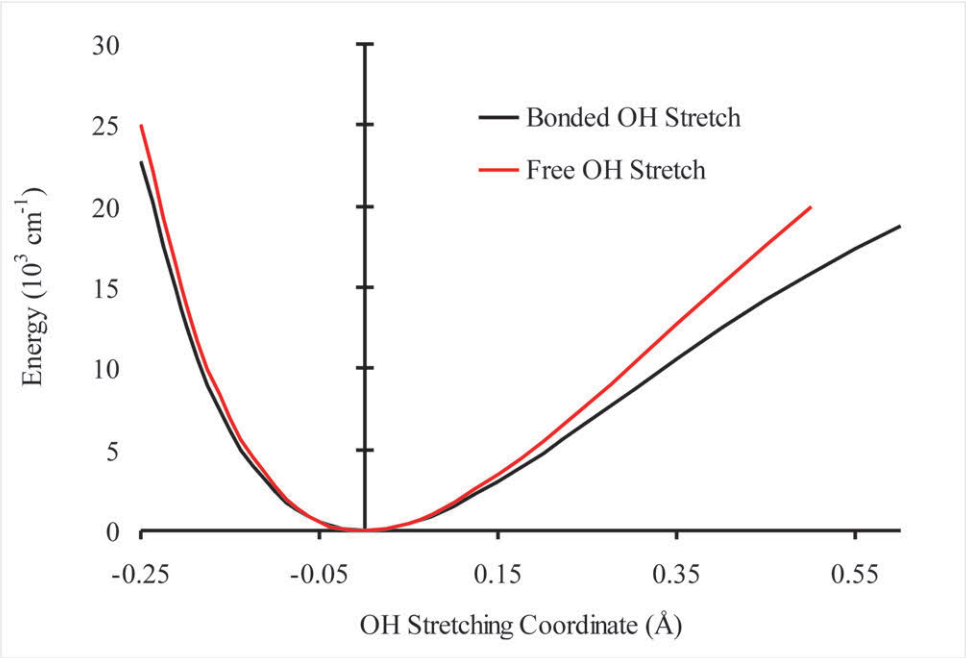

Figure 3.1: The One-dimensional OH stretching potential energy curve of the monomer unit 1 of the water trimer (see PAPER III) calculated using the CCSD(T)/aug-cc-pVTZ method. Å = 10^{-10} m.

The OH(O) stretching potential energy surface is symmetrical with respect to the O$\cdots$O bond [65].

3.1 What Happens When a Complex Is Formed?

The strongest feature in the absorption spectrum of the gas phase water is the fundamental HOH bending mode at 1594.7 cm^{-1}. The intensity of the overtone at 3151.6 cm^{-1} is significantly smaller the one of the fundamental. The two OH stretching oscillators are indistinguishable. These form a symmetric and an asymmetric combination. The local mode notation

$$\begin{aligned} |mn\rangle^{\pm} &= \tfrac{1}{\sqrt{2}}\left(|mn\rangle \pm |nm\rangle\right) \qquad m > n \\ |mn\rangle^{+} &= |mm\rangle \qquad\qquad\qquad\quad m = n, \end{aligned} \tag{3.1}$$

where m and n are the OH stretching quantum numbers, is commonly used to describe the OH stretching part of the wave function [66]. When it is

combined with the bending the total wave function becomes

$$|mn\rangle^{\pm}|v\rangle, \tag{3.2}$$

where v is the bending quantum number. The weak symmetric stretching fundamental is at 3657.1 cm^{-1}. The transition to the asymmetric $|10\rangle^{-}|0\rangle$ state is at 3755.9 cm^{-1}. It is almost as strong as the bending fundamental. In the OH stretching overtones, the asymmetric mode remains stronger than the corresponding symmetric transition. Another feature to note is that the energy difference between $|mn\rangle^{+}|v\rangle$ and $|mn\rangle^{-}|v\rangle$ decreases as $m + n$ increases.

In the donor unit of the water complex, the bending modes are slightly blueshifted. The hydrogen bond hinders the "off-O$\cdots$O-axis" motion of the bonded hydrogen atom. Therefore, the HOH angle bending potential energy surface becomes steeper and causes the blueshift in the HOH bending modes. The intensity of the fundamental decreases slightly and the first overtone becomes stronger. More radical changes appear in the OH stretching spectrum. As the OH oscillators are no longer equivalent, the interpretation for the state in Equation 3.1 is no longer valid. Therefore, a new notation is needed. The two OH stretching oscillators are non-equivalent and the wave function is

$$|m\rangle_{\mathrm{f}}|n\rangle_{\mathrm{b}}|v\rangle, \tag{3.3}$$

where the subscripts f and b refer to the free and bonded OH stretches, respectively. The true wave function is something between (3.2) and (3.3). For instance, in the case of the weakly bonded $H_2O\cdots NO$ complex, the fundamental OH stretching wave functions are[1] [PAPER IV]

$$0.77 \times |0\rangle_{\mathrm{f}}|1\rangle_{\mathrm{b}}|0\rangle + 0.63 \times |1\rangle_{\mathrm{f}}|0\rangle_{\mathrm{b}}|0\rangle \tag{3.4}$$

and

$$0.63 \times |0\rangle_{\mathrm{f}}|1\rangle_{\mathrm{b}}|0\rangle - 0.77 \times |1\rangle_{\mathrm{f}}|0\rangle_{\mathrm{b}}|0\rangle. \tag{3.5}$$

[1]The coefficients given in these examples are taken from the result of variational calculations. These are the coefficients of the basis functions that have the largest contribution to the total wave function of the given state. The OH stretching basis functions are the Morse oscillator eigenfunctions and the HOH bending basis functions are harmonic oscillator eigenfunctions. The potential energy parameters that were used to form the basis functions are given in PAPERS I and IV.

In a more strongly bound complex, the water dimer, the difference in between the coefficients of the free and bonded states is significantly larger [PAPER I]

$$0.92 \times |0\rangle_{\mathrm{f}}|1\rangle_{\mathrm{b}}|0\rangle + 0.36 \times |1\rangle_{\mathrm{f}}|0\rangle_{\mathrm{b}}|0\rangle \tag{3.6}$$

and

$$0.36 \times |0\rangle_{\mathrm{f}}|1\rangle_{\mathrm{b}}|0\rangle - 0.92 \times |1\rangle_{\mathrm{f}}|0\rangle_{\mathrm{b}}|0\rangle. \tag{3.7}$$

The harmonic force constant for the OH_b stretch is smaller than the one of the OH_f stretch. Therefore, the wavenumbers of the $|0\rangle_{\mathrm{f}}|n\rangle_{\mathrm{b}}|0\rangle$ transitions are smaller than the ones of $|n\rangle_{\mathrm{f}}|0\rangle_{\mathrm{b}}|0\rangle$, i.e., the OH_b transitions are redshifted. On the contrary to the water molecule, the energy difference increases as the vibrational quantum number increases.

3.2 The Intensities of the OH_b Stretching Modes

The water trimer intensities calculated in this work (Papers III and V) as well as the experimental Ne matrix ones [18] are presented in Table 3.1. The calculations reproduce well the intensities of all of the fundamental transitions in the water trimer. In the overtone region, the agreement between the calculated and the observed intensities is also good.

In a complex, the monomer units orient themselves so that their dipole moments are enhanced, especially the one involved in the OH_b stretching motion [67]. Therefore, the absorption intensities of the bonded OH stretching modes are in general stronger than the ones of the free OH stretches. All this is in concert with the previous observations of the medium-strength hydrogen bonded complexes [64]. The intensity increase, along with the redshift, makes the bonded OH stretches the most distinguished feature in the spectrum of the water complexes.

It is noteworthy to mention that in the case of the OH_b stretching coordinate the first and the second derivatives of the dipole moment function have the same sign unlike in the OH_f or the OH stretching coordinates in the water molecule. The most important terms, the one-dimensional part, in the oscillator strength calculation (see Equation 2.36) for the transition from the ground state to the first overtone are

$$\langle 2|\vec{\mu}|0\rangle \approx \vec{\mu}_1\langle 2|\Delta r_{\mathrm{b}}|0\rangle + \frac{1}{2}\vec{\mu}_2\langle 2|(\Delta r_{\mathrm{b}})^2|0\rangle, \tag{3.8}$$

Table 3.1: Comparison of calculated and experimental transition intensities for the water trimer. The strongest transition, ν_aOH_b, is scaled to 100. The symbol δ is the HOH bending mode, ν_sOH_b and ν_aOH_b are the symmetric and asymmetric OH_b stretching modes, respectively, and νOH_f is the OH_f stretching mode.

Transition	3×3D[a]	9D[b]	Exp.[18]
δ	15	15	17
2δ	2.0	1.9	1.4
ν_sOH_b		1.6	0.45
ν_aOH_b	100	100	100
νOH_f	18	19	14
3δ		0.073	0.045
$\nu_sOH_b + \delta$	2.2[c]	1.1	0.7
$\nu_aOH_b + \delta$		1.2	1.0
$\nu OH_f + \delta$	2.0	2.0	1.8
$\nu OH_b + 2\delta$	0.009	0.018	0.015
$2\nu OH_b$	0.11	0.08	0.09
$\nu OH_f + \nu OH_b$	0.39	0.40	0.36
$2\nu OH_f$	0.27	0.27	0.2

[a] The uncoupled model presented in Paper III.

[b] The coupled model presented in Paper V.

[c] The total intensity of the $\nu OH_b + \delta$ band. No symmetric/asymmetric split calculated using the uncoupled model.

keeping in mind that the oscillator strength of the absorption is proportional to $|\langle 2|\vec{\mu}|0\rangle|^2$. For a Morse oscillator with the parameter values $k = \frac{\omega}{\omega x} = 37.68$ and $a = 2.373$ Å^{-1} (the donor unit of the water dimer, PAPER I), the values of the integrals in Equation 3.8 are

$$\begin{aligned} \langle 2|\Delta r_b|0\rangle &= -8.22 \cdot 10^{-3} \quad \text{Å} \\ \langle 2|(\Delta r_b)^2|0\rangle &= 6.25 \cdot 10^{-3} \quad \text{Å}^2. \end{aligned} \tag{3.9}$$

Cancellation occurs due to different signs of the integrals. Hence, the value of the matrix element in Equation 3.8, and moreover the intensity of the first overtone is small. This phenomenon has been both observed [34] and calculated [47] in earlier studies of the water dimer.

The decrease in the intensity of the H-bonded OH stretching overtone

can be understood by using group theoretical arguments. Let us consider a triatomic $[F\cdots H\cdots F]^-$ ion where the hydrogen atom is located symmetrically between the fluorine atoms. Its symmetry point group is $D_{\infty h}$. The asymmetric FHF stretching mode, ν_3, corresponds to the hydrogen bonded stretch. The ground state is of A_{1g} symmetry as well as the first overtone of the stretching motion. The dipole moment spans $A_{1u} + E_{1u}$. The symmetry of the transition integrand, $\langle 2|\vec{\mu}|0\rangle$, in Equation 2.36 can be evaluated using group theory

$$A_{1g} \otimes (A_{1u} \oplus E_{1u}) \otimes A_{1g} = A_{1u} \oplus E_{1u} \neq A_{1g}. \tag{3.10}$$

Therefore, the intensity of the transition is equal to zero and the IR transition from the ground state to the first overtone is forbidden. The hydrogen bond in the water dimer is less symmetrical than the one in $[F\cdots H\cdots F]^-$, but still the overtone is noticeably weaker than the free OH stretching modes.

3.3 The Free OH Stretching Modes

A few points can be made about the free OH stretching modes:

1° The observed and calculated free OH stretching fundamentals are presented in Table 3.2. The adiabiatic model used in this work reproduces the transition wavenumber of the gas phase observation perfectly. Hence, the intermolecular modes are not needed to describe the free OH stretches.

2° The harmonic force constants of the water dimer OH stretching modes were calculated at various torsional angles in PAPER II. The ω parameter for the OH_f oscillator varies from 3927.73 to 3929.56 cm^{-1} during the torsional motion of the donor unit. This 1.83 cm^{-1} difference is small compared to the one of the OH_b mode, which is 15.10 cm^{-1}.

3° The vibrations of the water nitric oxide complex were studied in PAPER IV. The three lowest energy OH_b and OH_f stretching wavenumbers of two conformers (see Figure 1 in PAPER IV) are given in Table 3.3. In both, conformers the water molecule is hydrogen-bonded to the nitrogen atom of NO. Both conformers are planar. Conformer 1 becomes conformer 2 by rotating the water molecule by 180°. Even though there is a significant difference

Table 3.2: Observed and the variationally calculated (CCSD(T)/CBS+CV+rel) transition wavenumbers (in cm^{-1}) from PAPER I for the fundamental OH stretching modes in the proton donor unit of the water dimer in various environments.

Environment	$\|0\rangle_f\|1\rangle_b\|0\rangle$	$\|1\rangle_f\|0\rangle_b\|0\rangle$	Ref.
Gas Phase	3601	3735	[26]
He Droplet	3597	3729	[23]
Ne Matrix	3591	3734	[17]
Ar Matrix	3574	3708	[8]
Kr Matrix	3569		[15]
Calculated	3560	3735	This Work
N_2 Matrix	3550	3699	[7]
Xe Matrix	3531		[15]

Table 3.3: Variationally calculated fundamental OH stretching wavenumbers (in cm^{-1}) for the two $^2A'$ minimum energy conformers of the water nitric oxide complex. [PAPER IV]

Local Mode	Conformer 1	Conformer 2	Difference
$\|0\rangle_f\|1\rangle_b\|0\rangle$	3641.6	3645.1	3.5
$\|0\rangle_f\|2\rangle_b\|0\rangle$	7165.5	7175.0	9.5
$\|0\rangle_f\|3\rangle_b\|0\rangle$	10529.4	10547.5	18.1
$\|1\rangle_f\|0\rangle_b\|0\rangle$	3746.0	3748.2	2.2
$\|2\rangle_f\|0\rangle_b\|0\rangle$	7232.6	7235.2	2.6
$\|3\rangle_f\|0\rangle_b\|0\rangle$	10605.5	10606.0	0.5

in the bonded OH stretching energies of the two conformers, the free OH stretches remain almost unchanged. That is, even in the second overtone.

Based on these arguments, it can be concluded that the spatial orientation of the donor unit has little effect on the energies of free OH stretching modes.

3.4 Matrix Isolation Measurements of the Water Dimer

It is difficult to measure the band positions and the absorption intensities, especially the gas phase spectral data of water complexes. The size of the

water clusters can be controlled only up to a certain limit in the gas phase. Therefore, there are always water molecules present in the measurements. As the shifts in spectral position created by the complex formation are small in general, the absorptions of the water molecule and the complexes often overlap in the spectrum. Hence, it would be advantageous to perform the measurements in the absence of water. This has been done with the best success using the matrix isolation method. The amount of water can be controlled; different sized water complexes can be separated in the spectrum by altering the water concentration in the matrix. However, the matrix environment distorts the studied molecule. For instance, the redshifts in the OH stretching modes are larger in the matrix environment than in the gas phase.

As the molecule is contained, the vibrational motions are also somewhat hindered. Various observed term values, as well as the one calculated in this work, of the $|0\rangle_{\rm f}|1\rangle_{\rm b}|0\rangle$ and $|1\rangle_{\rm f}|0\rangle_{\rm b}|0\rangle$ transitions of the water dimer are presented in Table 3.2. In general, the matrix shift increases as the size of the matrix host atom increases. The greater the size is the more contained the trapped molecule is. The matrix shifts in the fundamentals of $OH_{\rm f}$ and $OH_{\rm b}$ are similar in magnitude.

Recently, the high-frequency spectrum up to the second OH stretching overtone region of the water dimer was observed in the Ne matrix [21]. The experimental spectrum of the acceptor unit was in a good agreement with the results in PAPER I. The largest difference between the observed and calculated energies was 18.5 $\rm cm^{-1}$. However, larger differences were observed in the donor unit. Even after the potential energy surface corrections[2], the hydrogen-bonded OH stretching modes were calculated lower in wavenumber than the experiments predicted. Some of the potential energy surface parameters were fitted with the non-linear least squares method using the experimental term values as the data. Observations from the fundamental OH stretching and HOH bending and their combination as well as the first OH stretching overtone regions were used in the fit. The least squares opti-

[2]Two different corrected potential energy surfaces were used. In the first one, the counterpoise correction [68] was applied on the CCSD(T)/aug-cc-pVQZ $OH_{\rm b}$ stretching surface. In the second one, the complete basis set limit expansion was used [69, 70] with the core-valence [55] and the relativistic [71] corrections. See PAPER I for the details.

mization of the parameters reduced the difference between the observed and calculated energies of the second OH_b stretching overtone from 102.7 to 25.5 cm^{-1}. That is, without using this observation in the fit.

3.5 The Water Trimer

The high-frequency spectrum of the water trimer has been calculated using two models. The calculated spectra from the fundamental OH_b is presented in Figure 3.2. The first one, in PAPER III, was done using the uncoupled Hamiltonian from Equation 2.33. In general, the agreement with the experiments was good, except for the overestimation of the redshift in the OH_b modes. This was corrected using a least squares optimization of the potential energy surface, as described in the previous section. However, a weak feature has been observed at approximately 50 cm^{-1} lower energy from the main peak of the OH_b fundamental [18]. The uncoupled model was unable to produce this feature. The intermolecular potential energy coupling, presented in Equation 2.33, was included into the model in PAPER V. It had little effect on the position of the band center, but the model was able to obtain a good estimate for the observed splitting as can be seen in Figure 3.2.

The calculated [PAPERS III & V] and observed [18] intensities of the water trimer high-frequency transitions are presented in Table 3.1. These intensities are not intensities of individual transitions, but sums of the peaks belonging to the given category of modes. This work and the matrix isolation results are in a good agreement. The difference between the coupled and uncoupled models is small. It is clear that the intermolecular coupling plays an unimportant role in the transition intensities of the high-frequency transitions.

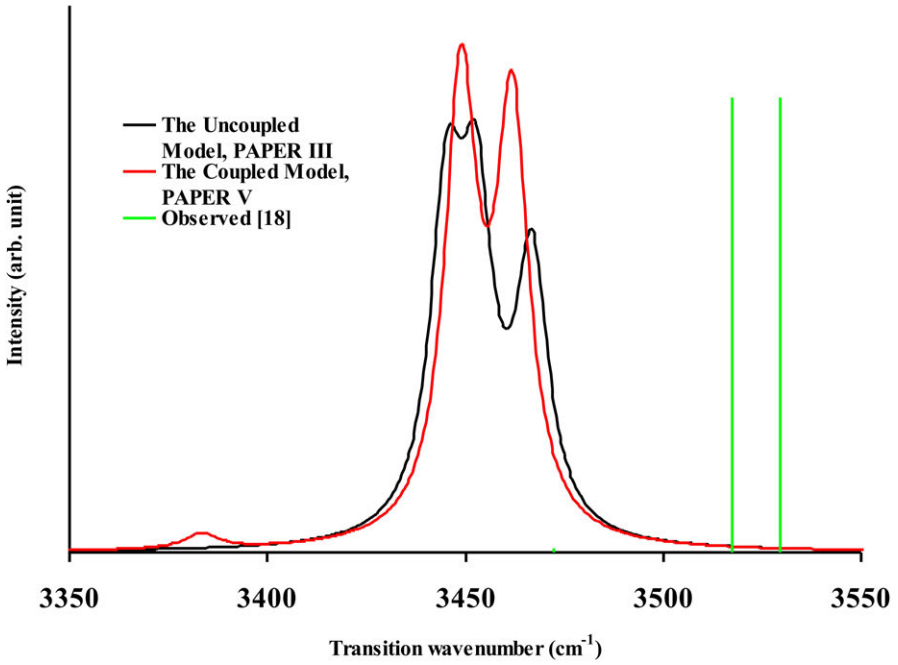

Figure 3.2: Calculated spectrum [CCSD(T)/aug-cc-pVTZ + CP correction] from the fundamental OH_b stretching region of the water trimer. The calculated spectra are convoluted using a Lorentzian band profile. The observed peaks are located at 3472.2 (very weak), 3517.5, and 3529.5 cm^{-1}. Only the total intensity of the high-energy doublet was given in Reference [18]. Hence, in this figure the total intensity is split into two equally intense peaks.

Chapter 4

Summary

The high-frequency vibrations of the water dimer, trimer, and nitric oxide complex have been studied in this thesis. I have utilized an adiabatic model, where the molecular complexes are treated as two or three individually vibrating monomer units. In the water dimer, the vibrational term values were calculated using a high-level ab initio method. I tested various corrections, in order to obtain a potential energy surface, which is sufficient for the purpose of this work. The adiabatic model worked well in most cases, but it slightly overestimated the redshift involved in the hydrogen-bonded OH stretching mode. A least squares optimization of some potential energy surface parameters using the gas phase and matrix isolation observations helped to overcome this problem. Most likely the inclusion of the most important low-frequency modes would improve the description of this vibrational mode. However, the model used in this work is a cost-efficient way to obtain the OH stretching overtone transition energies which are in a good agreement with experiments. The coupling of a low-frequency mode, the acceptor tunneling, with the OH stretching of the water dimer was also studied. These modes were coupled using an adiabatic model. A good estimate for the tunneling splitting of the vibrational ground state was obtained.

A model similar to the one used to calculate the high-frequency spectrum for the water dimer was also employed with the water nitric oxide complex. There were few computational studies, besides the harmonic normal mode calculation, about the complex before this work and a recent matrix isolation study in which three conformers were observed. The hydrogen bond in

H_2O–NO is much weaker than in the other complexes studied in this thesis. Therefore, the shifts are also smaller. Still, the calculations were able to confirm the assignments of the two conformers.

The water trimer OH stretching and HOH bending spectrum was calculated. First, the uncoupled model, which is similar to the one used with the water dimer, was used. Again, the agreement with the observations was reasonable, with the exception of the hydrogen-bonded OH stretching modes. The overestimation of the redshift was corrected with the least squares optimization of the potential energy surface. The result was good enough to propose some new assignments for the experimental spectrum. However, the shape of the bonded fundamental OH stretching band did not completely agree with the experiment. A new model, where the potential energy coupling between the monomer units was introduced, reproduced the observed band shape.

There is still some room for future improvements in this work. One possibility would be to include low-frequency modes in the water dimer calculation. This procedure could solve the problem related to the overestimation of the redshift in the hydrogen-bonded OH stretching mode. Another direction where this work can be continued is toward larger complexes. These include for instance, the water tetramer, pentamer, etc. Also other systems such as the complexes of water and small acid molecules such as HF or HCl could be studied using the models described in this thesis.

Bibliography

[1] V. F. Petrenko and R. W. Whitworth. *Physics of Ice*. Oxford University Press, Oxford, U. K., 2006.

[2] I. V. Ptashnik. *J. Quant. Spectrosc. Radiat. Transfer*, 109:831–852, 2008.

[3] R. Bukowski, K. Szalewicz, G. C. Groenenboom, and A. van der Avoird. *Science*, 315:1249–1252, 2007.

[4] O. Markovitch and N. Agmon. *Mol. Phys.*, 106:485–495, 2008.

[5] R. M. Bentwood, A. J. Barnes, and W. J. Orville-Thomas. *J. Mol. Spectrosc.*, 84:391–404, 1980.

[6] A. Engdahl and B. Nelander. *J. Chem. Phys.*, 86:4831–4837, 1987.

[7] J. P. Perchard. *Chem. Phys.*, 266:109–124, 2001.

[8] J. P. Perchard. *Chem. Phys.*, 273:217–233, 2001.

[9] P. G. Ayers and A. D. E. Pullin. *Spectrochimica Acta*, 32A:1629–1639, 1975.

[10] P. G. Ayers and A. D. E. Pullin. *Spectrochimica Acta*, 32A:1641–1650, 1975.

[11] P. G. Ayers and A. D. E. Pullin. *Spectrochimica Acta*, 32A:1689–1693, 1975.

[12] P. G. Ayers and A. D. E. Pullin. *Spectrochimica Acta*, 32A:1695–1704, 1975.

[13] J. Ceponkus, P. Uvdal, and B. Nelander. *J. Phys. Chem. A*, 112:3921–3926, 2008.

[14] K. Ohno, M. Okimura, N. Akai, and Y. Katsumoto. *Phys. Chem. Chem. Phys.*, 7:3005–3014, 2005.

[15] S. Hirabayashi and K. M. T. Yamada. *J. Chem. Phys.*, 122:244501, 2005.

[16] S. Hirabayashi and K. M. T. Yamada. *J. Mol. Struct.*, 795:78–83, 2006.

[17] Y. Bouteiller and J. P. Perchard. *Chem. Phys.*, 305:1 – 12, 2004.

[18] B. Tremblay, B. Madebène, M. E. Alikhani, and J. P. Perchard. *Chem. Phys.*, 378:27–36, 2010.

[19] N. Dozova, L. Krim, M. E. Alikhani, and N. Lacome. *J. Phys. Chem. A*, 110:11617–11626, 2006.

[20] J. Ceponkus, P. Uvdal, and B. Nelander. *J. Chem. Phys.*, 134:064309, 2011.

[21] Y. Bouteiller, B. Tremblay, and J. P. Perchard. *Chem. Phys.*, 386:29–40, 2011.

[22] R. Fröchtenicht, M. Kaloudis, M. Koch, and F. Huisken. *J. Chem. Phys.*, 105:6128–6140, 1996.

[23] C. J. Burnham, S. S. Xantheas, M. A. Miller, B. E. Applegate, and R. E. Miller. *J. Chem. Phys.*, 117:1109–1122, 2002.

[24] M. N. Slipchenko, K. E. Kuyanov, B. G. Sartakov, and A. F. Vilesov. *J. Chem. Phys.*, 124:241101, 2006.

[25] Z. S. Huang and R. E. Miller. *J. Chem. Phys.*, 91:6613–6631, 1989.

[26] F. Huisken, M. Kaloudis, and A. Kulcke. *J. Chem. Phys.*, 104:17–25, 1996.

[27] J. B. Paul, C. P. Collier, R. J. Saykally, J. J. Scherer, and A. O'Keefe. *J. Phys. Chem. A*, 101:5211–5214, 1997.

[28] J. B. Paul, R. A. Provencal, A. Petterson, and R. J. Saykally. *J. Chem. Phys.*, 109:10201–10206, 1998.

[29] J. B. Paul, R. A. Provencal, C. Chapo, A. Petterson, and R. J. Saykally. *J. Phys. Chem. A*, 103:2972–2974, 1999.

[30] M. R. Viant, J. D. Cruzan, D. D. Lucas, M. G. Brown, K. Liu, and R. J. Saykally. *J. Phys. Chem. A*, 101:9032–9041, 1997.

[31] M. R. Viant, M. G. Brown, J. D. Cruzan, R. J. Saykally, M. Geleijns, and A. van der Avoird. *J. Chem. Phys.*, 110:4369–4380, 1999.

[32] M. G. Brown, M. R. Viant, R. P. McLaughlin, C. J. Keoshian, E. Michael, J. D. Cruzan, R. J. Saykally, and A. van der Avoird. *J. Chem. Phys.*, 111:7789–7800, 1999.

[33] L. B. Braly, K. Liu, M. G. Brown, F. N. Keutch, R. S. Fellers, and R. J. Saykally. *J. Chem. Phys.*, 112:10314–10326, 2000.

[34] S. A. Nizkorodov, M. Ziemkiewicz, D. J. Nesbitt, and A. E. W. Knight. *J. Chem. Phys.*, 122:194316, 2005.

[35] A. F. A. Vilela, P. R. P. Barreto, R. Gargano, and C. R. M. Cunha. *Chem. Phys. Lett.*, 427:29–34, 2006.

[36] X. Huang, B. J. Braams, and J. M. Bowman. *J. Phys. Chem. A*, 110:445–451, 2006.

[37] K. Liu, J. D. Cruzan, and R. J. Saykally. *Science*, 271:929–933, 1996.

[38] N. A. Benedek, I. K. Snook, M. D. Towler, and R. J. Needs. *J. Chem. Phys.*, 125:104302, 2006.

[39] G. S. Tschumper, M. L. Leininger, B. C. Hoffman, E. F. Valeev, H. F. Schaefer III, and M. Quack. *J. Chem. Phys.*, 116:690–701, 2002.

[40] N. Goldman, R. S. Fellers, M. G. Brown, L. B. Braly, C. J. Keoshian, C. Leforestier, and R. J. Saykally. *J. Chem. Phys.*, 116:10148–10163, 2002.

[41] X. Huang, B. J. Braams, J. M. Bowman, R. E. A. Kelly, J. Tennyson, G. C. Groenenboom, and A. van der Avoird. *J. Chem. Phys.*, 128:034312, 2008.

[42] J. R. Lane and H. G. Kjaergaard. *J. Phys. Chem. A*, 131:034307, 2009.

[43] Y. Wang, S. Carter, B. J. Braams, and J. M. Bowman. *J. Chem. Phys.*, 128:071101, 2008.

[44] C. Leforestier, R. van Harrevelt, and A. van der Avoird. *J. Phys. Chem. A*, 113:12285–12294, 2009.

[45] Y. Wang and J. M. Bowman. *J. Chem. Phys.*, 134:154510, 2011.

[46] G. R. Low and H. G. Kjaergaard. *J. Chem. Phys.*, 110:9104–9115, 1999.

[47] D. P. Schofield and H. G. Kjaergaard. *Phys. Chem. Chem. Phys.*, 5:3100–3105, 2003.

[48] D. P. Schofield, J. R. Lane, and H. G. Kjaergaard. *J. Phys. Chem. A*, 111:567–572, 2007.

[49] H. G. Kjaergaard, A. L. Garden, G. M. Chaban, R. B. Gerber, D. A. Matthews, and J. F. Stanton. *J. Phys. Chem. A*, 112:4324–4335, 2008.

[50] T. Helgaker, P. Jørgensen, and J. Olsen. *Molecular Electronic-Structure Theory*. John Wiley & Sons, LTD, Chichester, UK, 2004.

[51] A. Szabo and N. S. Ostlund. *Modern Quantum Chemistry: Introduction to Advanced Electronic Structure Theory*. Dover, New York, 1996.

[52] P. V. Atkins. *Molecular Quantum Mechanics*. Oxford University Press, Oxford, 2 edition, 1983.

[53] T. H. Dunning, Jr. *J. Chem. Phys.*, 90:1007–1023, 1989.

[54] R. A. Kendall, T. H. Dunning Jr., and R. J. Harrison. *J. Chem. Phys.*, 96:6796–6806, 1992.

[55] D. E. Woon and T. H. Dunning, Jr. *J. Chem. Phys.*, 103:4572–4585, 1995.

[56] E. Sälli, T. Salmi, and L. Halonen. *J. Phys. Chem. A*, 115:11594–11605, 2011.

[57] J. Pesonen. *Application of geometric algebra to theoretical molecular spectroscopy.* PhD thesis, University of Helsinki, 2001.

[58] J. Pesonen. *J. Chem. Phys.*, 112:3121–3132, 2000.

[59] E. B. Wilson, J. C. Decius, and P. C. Cross. *Molecular Vibrations.* Dover, New York, 1980.

[60] P. M. Morse. *Phys. Rev.*, 34:57–64, 1929.

[61] G. Herzberg. *Molecular Spectra and Molecular Structure II.* Van Nostrand Reinhold Company, New York, 1 edition, 1945.

[62] A. J. Stone. *The Theory of Intermolecular Forces.* Oxford University Press, Oxford, UK, 2002.

[63] C. Eckart. *Phys. Rev.*, 47:552–558, 1935.

[64] M. D. Joesten and L. J. Schaad. *Hydrogen Bonding.* Marcel Dekker, Inc., New York, New York, 1974.

[65] M. E. Tuckerman, D. Marx, M. L. Klein, and M. Parrinello. *Science*, 275:817–820, 1997.

[66] L. Halonen. *Adv. Chem. Phys.*, 104:41–179, 1998.

[67] J. K. Gregory, D. C. Clary, K. Liu, M. G. Brown, and R. J. Saykally. *Science*, 275:814–817, 1997.

[68] S. F. Boys and F. Bernardi. *Mol. Phys.*, 19:553–566, 1970.

[69] A. Halkier, T. Helgaker, P. Jørgensen, W. Klopper, and J. Olsen. *Chem. Phys. Lett.*, 302:437–446, 1999.

[70] A. Halkier, T. Helgaker, P. Jørgensen, W. Klopper, H. Koch, J. Olsen, and A. K. Wilson. *Chem. Phys. Lett.*, 286:243–252, 1998.

[71] W. A. de Jong, R. J. Harrison, and D. A. Dixon. *J. Chem. Phys.*, 114:48–53, 2001.